Fibers **2015**, *3*, 338-347; doi:10.3390/fib3030338

OPEN ACCESS

fibers

ISSN 2079-6439

www.mdpi.com/journal/fibers

Article

Surface-Initiated Graft Atom Transfer Radical Polymerization of Methyl Methacrylate from Chitin Nanofiber Macroinitiator under Dispersion Conditions

Ryo Endo, Kazuya Yamamoto and Jun-ichi Kadokawa *

Graduate School of Science and Engineering, Kagoshima University, 1-21-40 Korimoto, Kagoshima 890-0065, Japan; E-Mails: k3406135@kadai.jp (R.E.); yamamoto@eng.kagoshima-u.ac.jp (K.Y.)

***** Author to whom correspondence should be addressed; E-Mail: kadokawa@eng.kagoshima-u.ac.jp; Tel.: +81-99-285-7743; Fax: +81-99-285-3253.

Academic Editor: Stephen C. Bondy

Received: 17 July 2015 / Accepted: 25 August 2015 / Published: 27 August 2015

Abstract: Surface-initiated graft atom transfer radical polymerization (ATRP) of methyl methacrylate (MMA) from self-assembled chitin nanofibers (CNFs) was performed under dispersion conditions. Self-assembled CNFs were initially prepared by regeneration from a chitin ion gel with 1-allyl-3-methylimidazolium bromide using methanol; the product was then converted into the chitin nanofiber macroinitiator by reaction with α-bromoisobutyryl bromide in a dispersion containing *N*,*N*-dimethylformamide. Surface-initiated graft ATRP of MMA from the initiating sites on the CNFs was subsequently carried out under dispersion conditions, followed by filtration to obtain the CNF-*graft*-polyMMA film. Analysis of the product confirmed the occurrence of the graft ATRP on the surface of the CNFs.

Keywords: atom transfer radical polymerization; chitin nanofiber; dispersion; methyl methacrylate; surface-initiated graft polymerization

---

1. Introduction

Chitin is a natural polysaccharide composed of β-(1→4)-linked *N*-acetyl-D-glucosamine units, and occurs mainly in the exoskeletons of crustaceans, shellfish, and insects [1–3]. Although chitin is one of the most abundant polysaccharides, it still remains as an unutilized biomass resource primarily because

of its intractable bulk structure and insolubility in common organic solvents and water due to the stiff polymer chain packing derived from numerous intra- and intermolecular hydrogen bonds. Therefore, studies on the conversion of chitin into functional bio-based materials, such as nanomaterials, by means of the proper dissolution, gelation, and processing have attracted much attention even in recent years [4–7].

To efficiently provide functional chitin materials through dissolution or gelation, we have focused on ionic liquids, which are low-melting-point salts that form liquids at temperatures below the boiling point of water, because they are identified as good solvents for natural polysaccharides such as cellulose [8–12]. Since it was first reported that an ionic liquid, 1-butyl-3-methylimidazolium chloride, dissolved cellulose [13], various ionic liquids have been used for the dissolution of cellulose and other polysaccharides [14–18]. We also found that the ionic liquid 1-allyl-3-methylimidazolium bromide (AMIMBr) dissolved chitin in concentrations up to *ca.* 4.8 wt% and further formed ion gels with higher contents of chitin [19,20]. We also reported in a subsequent publication that chitin self-assembled to form a nanofiber dispersion by regeneration from the ion gel using methanol [21,22]. When the dispersion was subjected to filtration, the isolated self-assembled chitin nanofibers (CNFs) entangled and formed a film.

We then investigated the surface-initiated graft polymerization of several monomers on the CNF films to give chitin-based composite materials [23–25]. For example, the surface-initiated graft atom transfer radical polymerization (ATRP) of 2-hydroxyethyl acrylate (HEA) on the surface of the CNF film, which carried covalently linked α-bromoisobutylate groups as the initiating sites (CNF macroinitiator film), was performed to produce the CNF-*graft*-polyHEA (CNF-*g*-PHEA) film [26]. SEM analysis confirmed that the film produced with shorter graft chains exhibited the nanofiber morphology, whereas the longer graft chains totally covered the surface of the film, resulting in the disappearance of the nanofiber morphology. This observation suggested that surface-initiated ATRP on the surface of the CNF film is not an efficient approach for the production of composite materials with CNF morphology and, thus, the resulting materials are not expected to exhibit the desirable CNF properties and functionality.

In this paper, we report surface-initiated graft ATRP of methyl methacrylate (MMA), a representative monomer polymerized by ATRP, on the surface of CNFs under dispersion conditions, followed by entanglement of the products to obtain CNF-based composite materials with nanofiber morphology (Figure 1). First, the initiating groups for ATRP were introduced by the reaction of α-bromoisobutyryl bromide with CNFs in the *N*,*N*-dimethylformamide (DMF) dispersion. Subsequently, the surface-initiated graft ATRP of MMA on the surface of the produced CNF macroinitiator in the dispersion was conducted, followed by filtration, to obtain the CNF-*graft*-polyMMA (CNF-*g*-PMMA) film with nanofiber morphology.

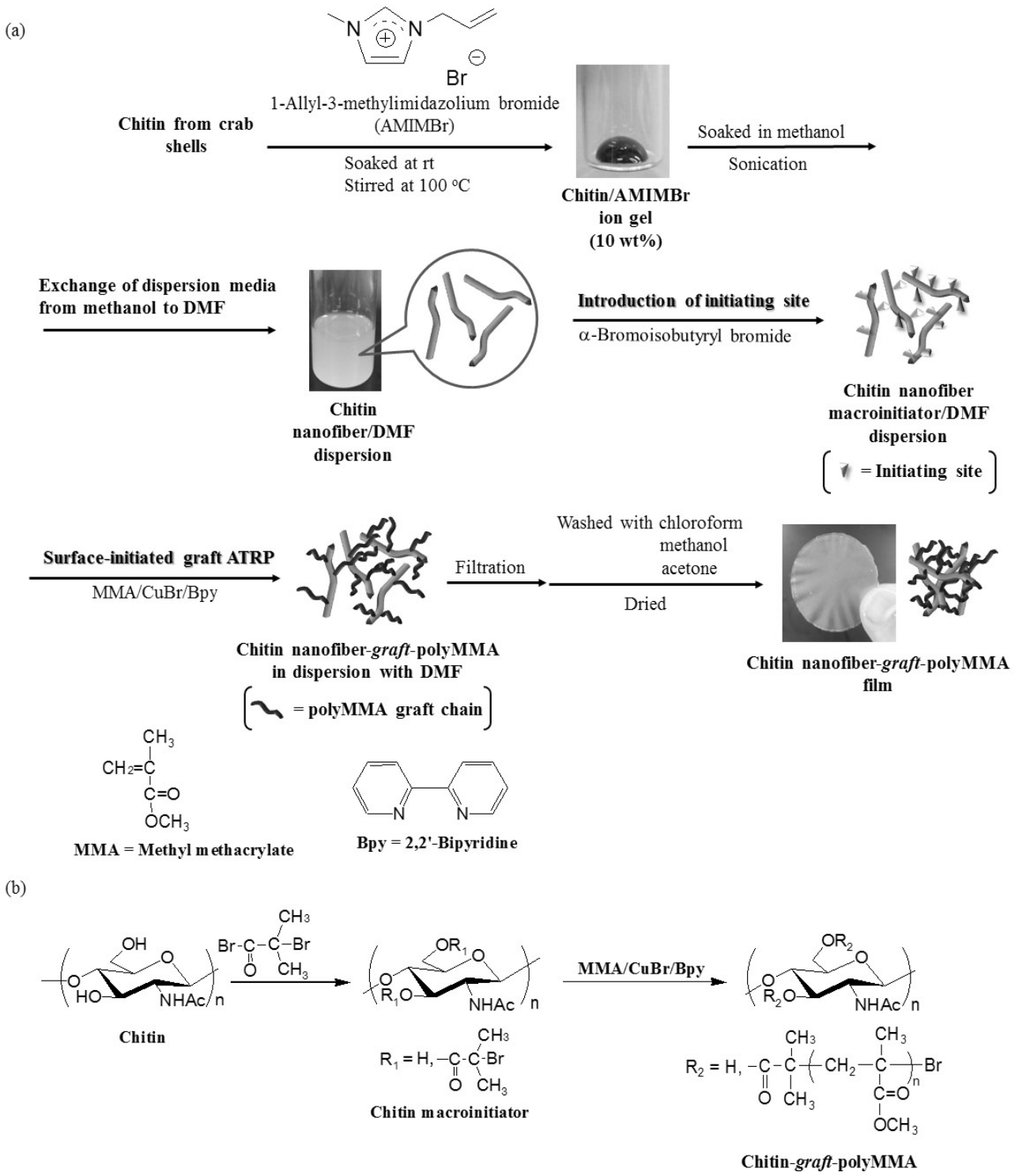

Figure 1. (**a**) Procedure for preparation of chitin nanofiber (CNF) macroinitiator in dispersion with DMF and surface-initiated graft ATRP of MMA under dispersion conditions; and (**b**) reaction scheme for chitin macroinitiator and chitin-*graft*-polyMMA (CNF-*g*-PMMA).

2. Experimental Section

2.1. Materials

Chitin powder from crab shells was purchased from Wako Pure Chemical Industries, Ltd., (Osaka, Japan). The weight-average molecular weight of the chitin sample was estimated to be 7×10^5 g/mol by viscometric analysis [27]. The ionic liquid AMIMBr was prepared by reaction of 1-methylimidazole with 3-bromo-1-propene according to the method previously published [28]. All other reagents and solvents were used as received from commercial sources.

2.2. Preparation of CNF Dispersion with DMF [21]

A mixture of chitin (0.120 g, 0.59 mmol) with AMIMBr (1.00 g, 4.92 mmol) was allowed to stand at room temperature for 24 h and subsequently heated with stirring at 100 ℃ for 24 h to obtain a chitin ion gel (10 wt%). The gel was then soaked in methanol (40 mL) at room temperature for 48 h, followed by sonication for 10 min to give self-assembled CNF dispersion with methanol. After addition of DMF (20 mL) to the dispersion, the mixture was evaporated at 60 ℃ for 2 h under reduced pressure to give the CNF dispersion with DMF (*ca.* 20 mL).

2.3. Preparation of CNF Macroinitiator in Dispersion with DMF

Pyridine (0.70 g, 8.85 mmol, 15 equiv. for a repeating unit of chitin) was mixed into the CNF dispersion with DMF (0.59 mmol/20 mL) and α-bromoisobutyryl bromide (2.71 g, 11.8 mmol, 20 equiv. for a repeating unit of chitin) was added dropwise with stirring at room temperature; the mixture was further stirred for 12 h to give the CNF macroinitiator dispersion with DMF. The CNF macroinitiator was isolated from the dispersion by filtration prior to characterization.

The resulting dispersion was subjected to centrifugation for 30 min and the supernatant containing the unreacted α-bromoisobutyryl bromide was removed. DMF (20–30 mL) was added and the procedure was repeated again in order to remove as much of the unreacted α-bromoisobutyryl bromide as possible.

2.4. Surface-Initiated Graft ATRP of MMA from CNF Macroinitiator in Dispersion with DMF

The typical experimental procedure for the surface-initiated ATRP was as follows. MMA (2.05 g, 20.5 mmol), copper(I) bromide (CuBr) (0.148 g, 1.03 mmol), and 2,2′-bipyridine (Bpy) (0.320 g, 2.05 mmol) (10, 0.5, and 1.0 equiv. for total initiating sites) were added to the CNF macroinitiator dispersion with DMF (total initiating sites (which were covalently linked on CNF + residual α-bromoisobutyryl bromide) = 2.05 mmol). The mixture was then incubated at 60 ℃ for 24 h and filtered. The resulting residue was washed with chloroform, methanol, and acetone and dried under reduced pressure to obtain the CNF-*g*-PMMA film (0.117 g).

2.5. Methods

IR spectra were recorded on a PerkinElmer Spectrum Two spectrometer using KBr pellets of the samples (resolution; 4 cm^{-1}, number of scans: 16). The SEM images of the platinum-coated samples were obtained using a Hitachi S-4100H electron microscope by applying 5 kV acceleration voltage. Prior

to acquisition of the SEM images, the samples were first placed on glass plates, followed by coating with platinum using magnetron splutter. Powder X-ray diffraction (XRD) measurements of the samples on glass plates were conducted using a PANalytical X'Pert Pro MPD with Ni-filtered CuK α radiation (λ = 0.15418 nm, dwell time; 0.05 s). The ^{1}H NMR spectrum was recorded on a JEOL ECX 400 spectrometer. The stress-strain curves were measured using a tensile tester (Little Senstar LSC-1/30, Tokyo Testing Machine, Tokyo, Japan).

3. Results and Discussion

As previously reported [21], the CNF dispersion in methanol was prepared via gelation with AMIMBr, followed by regeneration using methanol as shown in Figure 1a. For graft ATRP on CNFs under dispersion conditions, we then attempted to synthesize the CNF macroinitiator by the reaction of α-bromoisobutyryl bromide with the hydroxy groups on the CNFs. Because it was obvious that α-bromoisobutyryl bromide would react with the solvent present in the dispersion, thereby resulting in inhibition of the reaction with CNFs, it was necessary to exchange the dispersion medium by removal of methanol and addition of other liquids that do not react with α-bromoisobutyryl bromide. Accordingly, some liquids with relatively high boiling points, e.g., DMF, *N*,*N*-dimethylacetamide (DMAc), and dimethylsulfoxide (DMSO), were respectively added to the CNF dispersion with methanol and the resulting mixtures were evaporated to remove methanol. Consequently, in the mixture with DMF, chitin remained in the dispersed state after several hours, whereas in the other two mixtures with DMAc and DMSO, chitin underwent aggregation. Indeed, the nanofiber morphology is observed in the SEM image of the resulting dispersion with DMF (Figure 2b), which is the same as that in the original dispersion with methanol (Figure 2a).

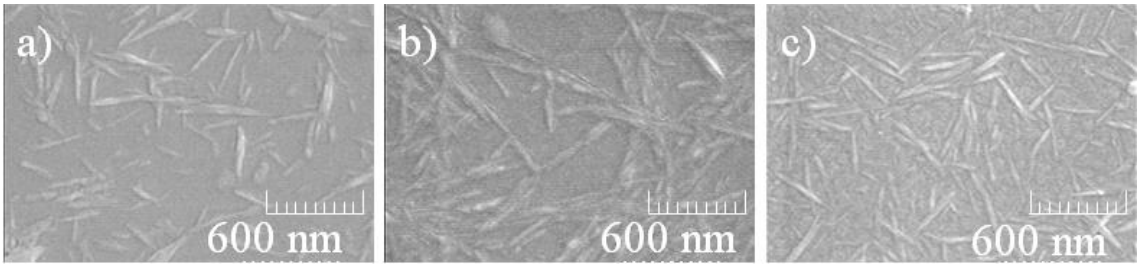

Figure 2. (**a**) SEM images of CNF dispersion with methanol; (**b**) CNF dispersion with DMF; and (**c**) CNF macroinitiator dispersion with DMF.

The reaction of α-bromoisobutyryl bromide (20 equiv. for a repeating unit of chitin) with the hydroxy groups on CNF in the dispersion with DMF was carried out in the presence of pyridine to produce the CNF macroinitiator (Figure 1b). The SEM image of the dispersion after the reaction suggests retention of the nanofiber morphology of chitin (Figure 2c). The detection of an ester group carbonyl absorption at 1730 cm^{-1} in the IR spectrum of the CNF macroinitiator (Figure 3a), which was isolated from the dispersion by filtration, strongly supported the presence of α-bromoisobutylate initiating sites on the CNFs. From the intensity ratio of the two carbonyl absorptions due to ester and amide I (1730 and 1660 cm^{-1}, respectively) in the IR spectrum, the functionality of the initiating sites on CNFs was estimated to be 0.37 for a repeating unit of chitin according to a method documented in the literature [29].

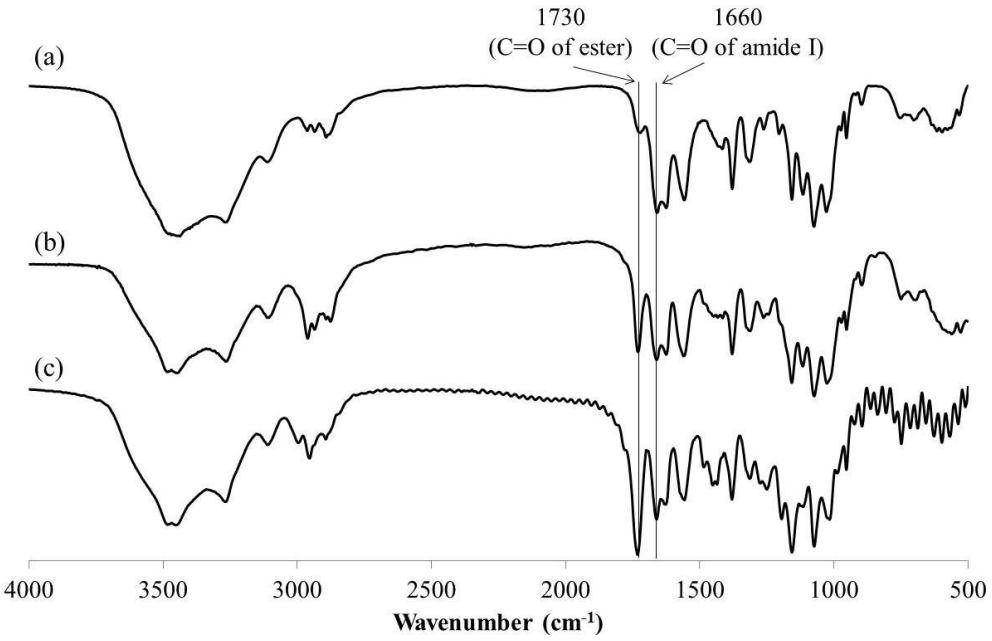

Figure 3. IR spectra of CNF macroinitiator (**a**) and CNF-*g*-PMMA films (MMA; 5 equiv. (**b**); 10 equiv. (**c**)).

Prior to surface-initiated graft ATRP, as much of the unreacted α-bromoisobutyryl bromide as possible was removed from the CNF dispersion by repeated centrifugation. The amount of removed α-bromoisobutyryl bromide was estimated by ^{1}H NMR analysis of the supernatant after centrifugation in $CDCl_3$ using 1,4-dimethoxybenzene as an internal standard. On the basis of this estimation, the total initiating sites (that were covalently linked on CNF and residual α-bromoisobutyryl bromide) in the dispersion with DMF (*ca.* 20 mL) were calculated to be *ca.* 2 mmol. Surface-initiated graft ATRP of MMA (5 and 10 equiv. for an initiating site) from the CNF macroinitiator was carried out in the presence of CuBr and BPy (0.5 and 1.0 equiv. for an initiating site, respectively) in the dispersion with DMF at 60 ℃ for 24 h (Figure 1a,b). The resulting materials were isolated by filtration, washed with chloroform, methanol, and acetone, and dried under reduced pressure to give CNF-*g*-PMMA films. The intensity ratios of the ester absorption to the amide I absorption in the IR spectra of the products (Figure 3b,c) increased in comparison to that of the CNF macroinitiator film (Figure 3a), suggesting the successful graft polymerization of MMA. In addition, the intensity of the ester absorption in the IR spectra was higher when 10 equiv. of MMA was used than when 5 equiv. was used, indicating that longer graft chains were produced in the former case.

The SEM images of the resulting films show the nanofiber morphologies (Figure 4b,c). The images also indicate that the nanofibers are merged at the interfacial areas, and are thus completely different from those of the original CNF film (Figure 4a). As we previously reported, on the other hand, the SEM image of the CNF-*g*-PHEA film (which was produced by surface-initiated graft ATRP on the film) does not show the nanofiber morphology (Figure 4d) [26]. These results suggest that in the present study, surface-initiated graft ATRP occurs on the surface of each nanofiber under dispersion conditions. Thus, the nanofibers become entangled during filtration and are merged among the non-crystalline PMMA graft chains on the nanofibers. The occurrence of the graft ATRP on the surface of the CNFs only was also supported by the XRD data given that the XRD pattern of the resulting film (Figure 5b) is the same

as that of the original CNF film (Figure 5a), indicating no disruption of the chitin crystalline structure after ATRP. Because the two XRD profiles are almost identical, it can be deduced that there was no significant change in the crystallinity after ATRP.

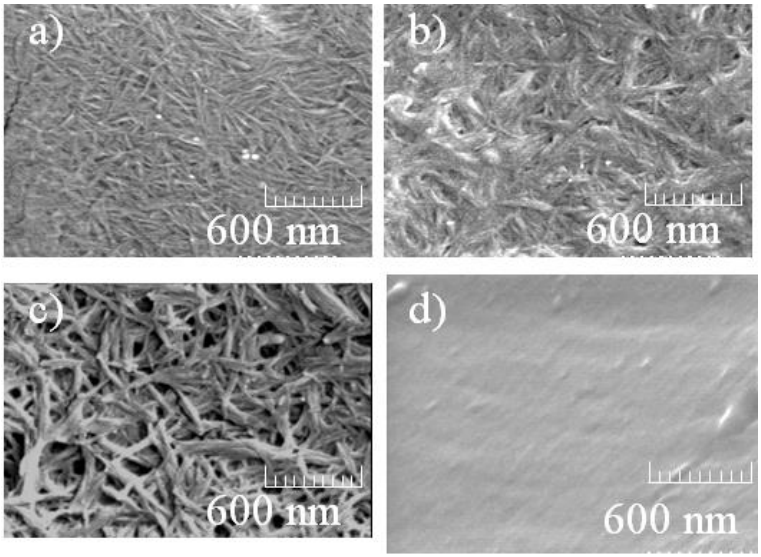

Figure 4. SEM images of CNF film (**a**); CNF-*g*-PMMA films (MMA; 5 equiv. (**b**); 10 equiv. (**c**)); and CNF-*g*-PHEA film ((**d**), HEA; 20 equiv. for an initiating site, conversion; 71%).

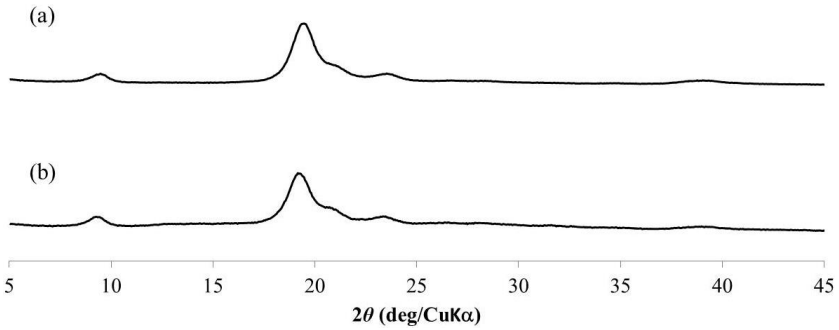

Figure 5. XRD patterns of CNF film (**a**) and CNF-*g*-PMMA film ((**b**), MMA; 10 equiv.).

The mechanical property of the resulting CNF-*g*-PMMA film was evaluated by tensile testing. Figure 6 shows a comparison of the stress-strain curve of the CNF-*g*-PMMA film obtained using 5 equiv. of MMA *versus* that of the original CNF and PMMA films. The elongation at break value of the CNF-*g*-PMMA film is slightly larger than that of the original CNF film (1.3% *versus* 1.1%), whereas the tensile strength of the former was lower than that of the latter (12.2 and 16.1 MPa) (Figure 6a,b). The presence of the graft PMMA chains in the CNF-*g*-PMMA film contributes to the observed change in the mechanical property because the PMMA film exhibits a highly elastic nature as shown in Figure 6c.

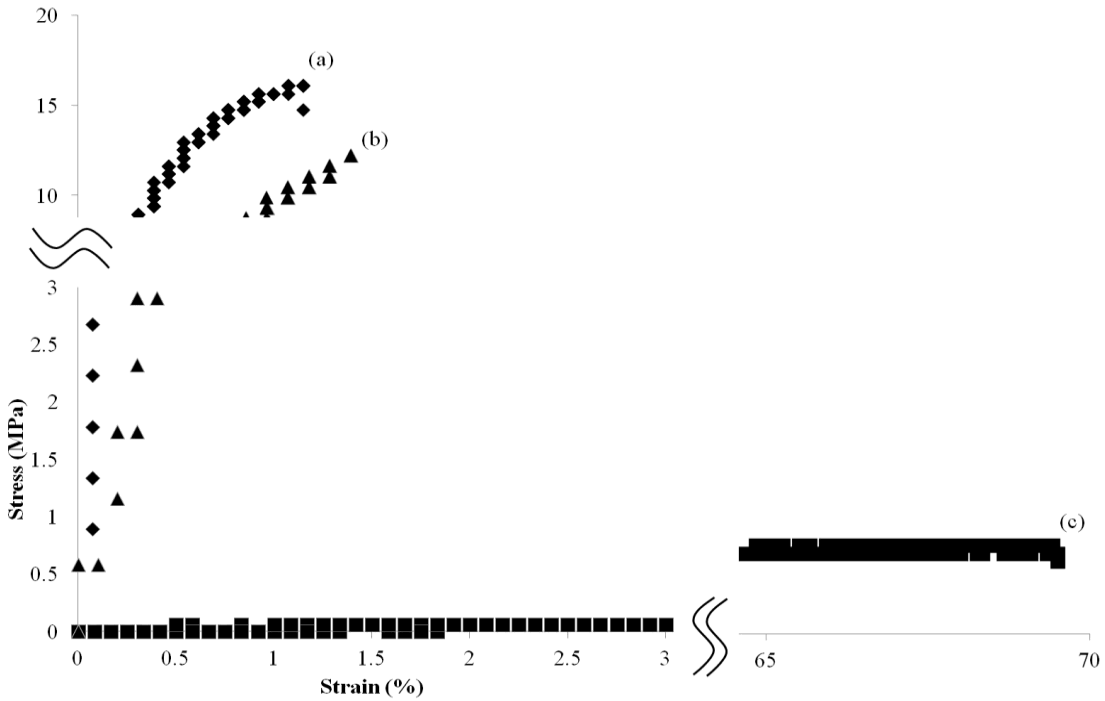

Figure 6. Stress-strain curves of CNF film (**a**); CNF-*g*-PMMA film ((**b**), MMA; 5 equiv.); and PMMA film (**c**).

4. Conclusions

In this study, surface-initiated graft ATRP of MMA was carried out on the surface of CNFs under dispersion conditions. The CNF dispersion with methanol was first prepared from the chitin ion gel with AMIMBr according to the regeneration procedure previously reported by the present authors. The protocol involves the exchange of the dispersion media by the removal of methanol and the introduction of DMF, after which the initiating sites for ATRP were introduced by the reaction of α-bromoisobutyryl bromide with hydroxy groups on the surface of the CNFs in the dispersion to obtain the CNF macroinitiator dispersion with DMF. The surface-initiated graft ATRP of MMA (5, 10 equiv. for an initiating site) was then performed in the presence of CuBr and Bpy at 60 ℃ under dispersion conditions. The products were isolated by filtration to produce the CNF-*g*-PMMA films. The presence of CNFs in the films was confirmed from the IR spectra, which also suggested the production of longer graft chains when a higher feed equiv. of MMA was utilized. The SEM images of the films confirmed the nanofiber morphology, which also indicated that nanofibers were merged at interfacial areas. The occurrence of the graft ATRP on the surface of the CNFs was further supported by XRD measurements. The mechanical property of the CNF-*g*-PMMA film was evaluated by tensile testing. The present products are new CNF-based composite materials and, accordingly, have the potential to be used as eco-friendly and environmentally benign materials in practical applications.

Author Contributions

Jun-ichi Kadokawa conceived the project and designed the experiments. Jun-ichi Kadokawa and Kazuya Yamamoto directed the research. Ryo Endo performed the experiments. Jun-ichi Kadokawa wrote the manuscript. All authors discussed the results and edited the manuscript.

Conflicts of Interest

The authors declare no conflict of interest.

References

1. Kurita, K. Chitin and chitosan: Functional biopolymers from marine crustaceans. *Mar. Biotechnol.* **2006**, *8*, 203–226.
2. Rinaudo, M. Chitin and chitosan: Properties and applications. *Prog. Polym. Sci.* **2006**, *31*, 603–632.
3. Pillai, C.K.S.; Paul, W.; Sharma, C.P. Chitin and chitosan polymers: Chemistry, solubility and fiber formation. *Prog. Polym. Sci.* **2009**, *34*, 641–678.
4. Muzzarelli, R.A.A. New techniques for optimization of surface area and porosity in nanochitins and nanochitosans. *Adv. Polym. Sci.* **2011**, *244*, 167–186.
5. Muzzarelli, R.A.A. Biomedical exploitation of chitin and chitosan via mechano-chemical disassembly, electrospinning, dissolution in imidazolium ionic liquids, and supercritical drying. *Mar. Drugs* **2011**, *9*, 1510–1533.
6. Muzzarelli, R.A.A.; El Mehtedi, M.; Mattioli-Belmonte, M. Emerging biomedical applications of nano-chitins and nano-chitosans obtained via advanced eco-friendly technologies from marine resources. *Mar. Drugs* **2014**, *12*, 5468–5502.
7. Kadokawa, J. Fabrication of nanostructured and microstructured chitin materials through gelation with suitable dispersion media. *RSC Adv.* **2015**, *5*, 12736–12746.
8. Liebert, T.; Heinze, T. Interaction of ionic liquids with polysaccharides 5. Solvents and reaction media for the modification of cellulose. *Bioresources* **2008**, *3*, 576–601.
9. Feng, L.; Chen, Z.I. Research progress on dissolution and functional modification of cellulose in ionic liquids. *J. Mol. Liq.* **2008**, *142*, 1–5.
10. Pinkert, A.; Marsh, K.N.; Pang, S.S.; Staiger, M.P. Ionic liquids and their interaction with cellulose. *Chem. Rev.* **2009**, *109*, 6712–6728.
11. Gericke, M.; Fardim, P.; Heinze, T. Ionic liquids—Promising but challenging solvents for homogeneous derivatization of cellulose. *Molecules* **2012**, *17*, 7458–7502.
12. Isik, M.; Sardon, H.; Mecerreyes, D. Ionic liquids and cellulose: Dissolution, chemical modification and preparation of new cellulosic materials. *Int. J. Mol. Sci.* **2014**, *15*, 11922–11940.
13. Swatloski, R.P.; Spear, S.K.; Holbrey, J.D.; Rogers, R.D. Dissolution of cellose with ionic liquids. *J. Am. Chem. Soc.* **2002**, *124*, 4974–4975.
14. El Seoud, O.A.; Koschella, A.; Fidale, L.C.; Dorn, S.; Heinze, T. Applications of ionic liquids in carbohydrate chemistry: A window of opportunities. *Biomacromolecules* **2007**, *8*, 2629–2647.
15. Zakrzewska, M.E.; Bogel-Łukasik, E.; Bogel-Łukasik, R. Solubility of carbohydrates in ionic liquids. *Energy Fuels* **2010**, *24*, 737–745.
16. Wang, W.T.; Zhu, J.; Wang, X.L.; Huang, Y.; Wang, Y.Z. Dissolution behavior of chitin in ionic liquids. *J. Macromol. Sci. B Phys.* **2010**, *49*, 528–541.
17. Jaworska, M.M.; Kozlecki, T.; Gorak, A. Review of the application of ionic liquids as solvents for chitin. *J. Polym. Eng.* **2012**, *32*, 67–69.

18. Kadokawa, J. Ionic liquid as useful media for dissolution, derivatization, and nanomaterial processing of chitin. *Green Sustain. Chem.* **2013**, *3*, 19–25.
19. Yamazaki, S.; Takegawa, A.; Kaneko, Y.; Kadokawa, J.; Yamagata, M.; Ishikawa, M. An acidic cellulose-chitin hybrid gel as novel electrolyte for an electric double layer capacitor. *Electrochem. Commun.* **2009**, *11*, 68–70.
20. Prasad, K.; Murakami, M.; Kaneko, Y.; Takada, A.; Nakamura, Y.; Kadokawa, J. Weak gel of chitin with ionic liquid, 1-allyl-3-methylimidazolium bromide. *Int. J. Biol. Macromol.* **2009**, *45*, 221–225.
21. Kadokawa, J.; Takegawa, A.; Mine, S.; Prasad, K. Preparation of chitin nanowhiskers using an ionic liquid and their composite materials with poly(vinyl alcohol). *Carbohydr. Polym.* **2011**, *84*, 1408–1412.
22. Tajiri, R.; Setoguchi, T.; Wakizono, S.; Yamamoto, K.; Kadokawa, J. Preparation of self-assembled chitin nanofibers by regeneration from ion gels using calcium halide dihydrate/methanol solutions. *J. Biobased Mater. Bioenergy* **2013**, *7*, 655–659.
23. Setoguchi, T.; Yamamoto, K.; Kadokawa, J. Preparation of chitin nanofiber-graft-poly (L-lactide-co-e-caprolactone) films by surface-initiated ring-opening graft copolymerization. *Polymer* **2012**, *53*, 4977–4982.
24. Kadokawa, J.; Setoguchi, T.; Yamamoto, K. Preparation of highly flexible chitin nanofiber-graft-poly(g-L-glutamic acid) network film. *Polym. Bull.* **2013**, *70*, 3279–3289.
25. Yamamoto, K.; Yoshida, S.; Mine, S.; Kadokawa, J. Synthesis of chitin-graft-polystyrene via atom transfer radical polymerization initiated from a chitin macroinitiator. *Polym. Chem.* **2013**, *4*, 3384–3389.
26. Yamamoto, K.; Yoshida, S.; Kadokawa, J. Surface-initiated atom transfer radical polymerization from chitin nanofiber macroinitiator film. *Carbohydr. Polym.* **2014**, *112*, 119–124.
27. Poirier, M.; Charlet, G. Chitin fractionation and characterization in n,n-dimethylacetamide/lithium chloride solvent system. *Carbohydr. Polym.* **2002**, *50*, 363–370.
28. Zhao, D.B.; Fei, Z.F.; Geldbach, T.J.; Scopelliti, R.; Laurenczy, G.; Dyson, P.J. Allyl-functionalised ionic liquids: Synthesis, characterisation, and reactivity. *Helv. Chim. Acta.* **2005**, *88*, 665–675.
29. Ando, T.; Kataoka, S. Acylation of chitin with acid anhydrides in trichloroacetic acid systems. *Kobunshi Ronbunshu* **1980**, *37*, 1–7.